IEEE Access
Multidisciplinary ⋮ Rapid Review ⋮ Open Access Journal

Received October 18, 2017, accepted December 12, 2017, date of publication December 18, 2017,
date of current version March 12, 2018.

Digital Object Identifier 10.1109/ACCESS.2017.2784801

Printed Ridge Gap Waveguide 3-dB Coupler: Analysis and Design Procedure

MOHAMED MAMDOUH M. ALI, (Student Member, IEEE),
SHOUKRY I. SHAMS, (Member, IEEE), AND ABDEL-RAZIK SEBAK, (Fellow, IEEE)
Electrical and Computer Engineering Department, Concordia University, Montreal, QC H4B 1R6, Canada

Corresponding author: Mohamed Mamdouh M. Ali (mohamed.ali@ieee.org)

ABSTRACT Communication systems are witnessing an outstanding revolution that has a clear impact on all aspects of life. The world technology is drifting towards high frequency and data rate solutions to accommodate the future expansion in applications such as 5G communications. The 5G technology will offer advanced features in the mm-Wave frequency band which requires intelligent subsystems such as beam switching. Therefore, the microwave components, especially couplers, still need a significant improvement to follow the rapid variations in future technologies. One of the most recent and promising guiding technologies for mm-Wave applications is the printed ridge gap waveguide (PRGW). In this paper, a design of 3-dB planar quadrature hybrid coupler based on PRGW is presented. The proposed design has superior characteristics such as compactness, low loss, and low dispersion device. The prototype of the proposed coupler is fabricated and tested, where the measured and simulated results show an excellent agreement.

INDEX TERMS Hybrid coupler, printed ridge gap waveguide, periodic structures.

I. INTRODUCTION

The 5G communication system is one of the most promising standards in the future. This standard is featured with its ability to accommodate a huge number of connected devices with low latency, high data rate, and reliable connection [1]. Many applications are predicted for 5G to enhance the existing 4G use cases as well as some new and emerging applications. Therefore, a new frequency band may be required to achieve the target performance of 5G. The mobile industry is envisaged to extend mobile services into spectrum bands in the range above 6 GHz to gain additional bandwidth of several GHz. As the results, various regulators such as the United States Federal Communications Commission (FCC), in October 2014, have been investigating several bands as a potential for 5G based on technical matters and licensing options. One of these bands is local multipoint distribution service (LMDS) band which is divided into several subbands with 1 GHz of spectrum that would be required for the initial deployment of a local multipoint communications system (LMCS) in the 30 GHz band [1]–[3].

However, the realization of the 5G communication system is limited by the availability of various components with superior electrical performance, especially in mm-wave range [4]. The 5G systems will be limited also by the availability of smart subsystems such as beam switching to improve the reliability of communication links. These subsystems highlight the directional couplers as they are deployed in building both the power dividers and the crossovers. Directional couplers are essential devices in any microwave systems to extract a directive sample from the input power [5]. They can be realized based either on traditional technologies such as microstrip line [6], [7] and stripline [8], [9]. In addition, they can be implemented by the modern guiding structures such as substrate integrated waveguide (SIW) realization [10]–[18]. The guiding structures technology has a tangible revolution that encourages the research community to exert more effort in providing new solutions accommodating the state of the art structures. One of the promising guiding structures suitable for high-frequency band applications is the ridge gap waveguide (RGW). The RGW is introduced for the first time in 2009 as a TEM guiding structure and developed in the printed version in 2012 which called printed ridge gap waveguide (PRGW) [19], [20]. They are considered among the most important candidates for the 5G system due to low signal distortion as the propagating mode is a quasi-TEM mode. Another advantage of this guiding structure is the relatively low loss at mm-wave frequencies since the wave propagates inside an air gap. Due to the importance of such structure, many designs were introduced in the literature such as filter and antennas [22], [23], [25], [26]. However, as a recently invented guiding structure, there is still a large room for designing directional couplers as they are visited a few times in the literature [21], [24].

This paper presents the design and the implementation of a PRGW hybrid directional coupler for 5G communication applications centered at 30 GHz. The 5G final standard is not released yet, however, it is expected to utilize different frequency bands with frequencies above 6 GHz has approximately a 5% average bandwidth per band [1]–[3]. Moreover, the center frequency of each band will vary from country to another [1]. Although the presented design is centered at 30 GHz, it is simple and straightforward to apply the proposed procedure and redesign at different bands.

The main contribution of this paper is to introduce a coupling mechanism that provides a flat 3 dB forward coupling with superior electrical characteristics in a mm-wave frequency band. The proposed coupler is featured with its compactness that enables the integration with other components and reduces the overall system cost. Moreover, it has a 6% percentage bandwidth which able to cover the operating bandwidth of 5G applications. Furthermore, the proposed device is implemented based on a PRGW technology that supports a quasi-TEM mode, which minimizes the signal distortion.

This paper is organized as follows: Section II presents the design procedure to implement a 3-dB coupler. In section III, we present the microstrip to PRGW transition required to validate the proposed devices experimentally. Prototype and measured results of the proposed devices are presented in Section IV. Finally, Section V introduces a summary of the paper outcomes and suggests the future expansion of this work.

II. PRGW QUADRATURE HYBRID COUPLER

The proposed coupler will be designed through four steps; the first step is to select the proper dimensions for the periodic unit cell surrounding the ridge to suppress any leakage centered at 30 GHz and covers more than 5% bandwidth required for the 5G application. The second step is a precise strip line model for the PRGW line constructed using the pre-designed unit cell. Afterwards, the design procedure for calculating the coupling section dimensions is proposed and illustrated. Finally, a fine tuning process is performed in order to achieve the required electrical characteristics over the operating bandwidth.

A. DESIGN OF UNIT CELL AND PRGW LINE

The geometrical configuration of the printed ridge gap waveguide and EBG unit cell are shown in Figure 1(a) and 1(b), respectively. The unit cell is printed on Roger RT 6002 with dielectric constant ($\varepsilon_r = 2.94$) and substrate thickness ($h_s = 0.508$ mm). Many articles have discussed the cell design procedure and the associated realized bandwidth [24], [26]. Through the published design procedure, it is straightforward to obtain the cell dimensions

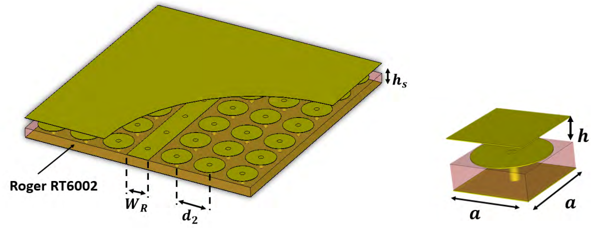

(a) (b)

FIGURE 1. The geometrical configuration of (a) PRGW. (b) EBG unit cell.

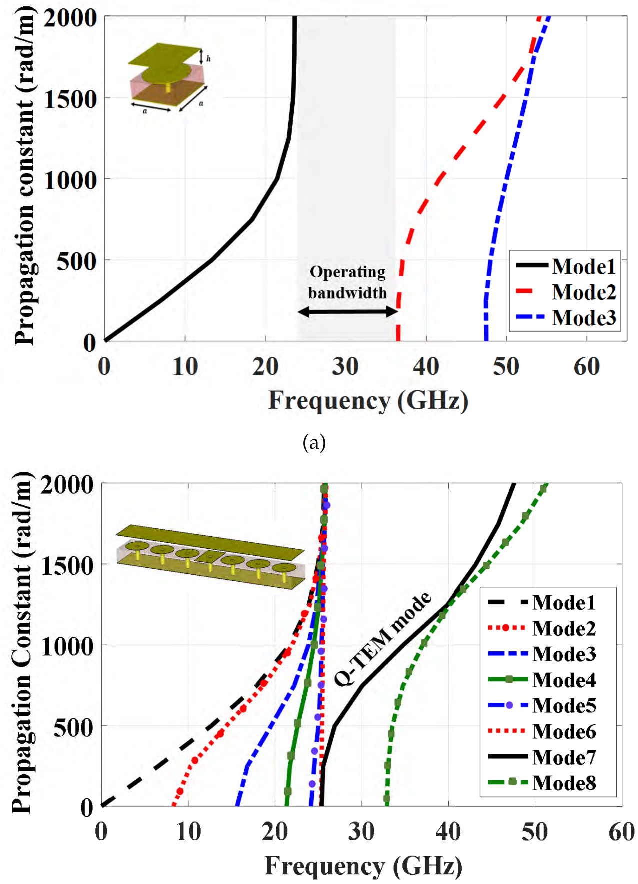

(a)

(b)

FIGURE 2. Dispersion diagram of (a) EBG unit cell and (b) PRGW section.

listed in Table 1. The simulated dispersion diagram of a unit cell, designed to cover the 23.5-36.5 GHz frequency band, is shown in Figure 2(a). The proposed unit cell provides a 33.3% relative bandwidth which is wider than required for 5G applications.

The propagating quasi-TEM mode is supported by adding the guiding ridge in the center of the EBG structures. However, the realized bandwidth of the cell is affected by adding the ridge as shown in [29, Fig. 2(b)]. The ridge width and separation of the first row of cells are mentioned in Table 1 as well. The guiding ridge is provided with via holes in the ground plane. They have the same period d_2 that is equal to

TABLE 1. Dimensions of the printed ridge GAP waveguide.

Variable	Value in (mm)
Gap height (h)	0.508
Substrate height (h_s)	0.508
Cell size (a)	1.7
Ridge width (W_R)	1.5
Unit cell period (d_2)	1.85

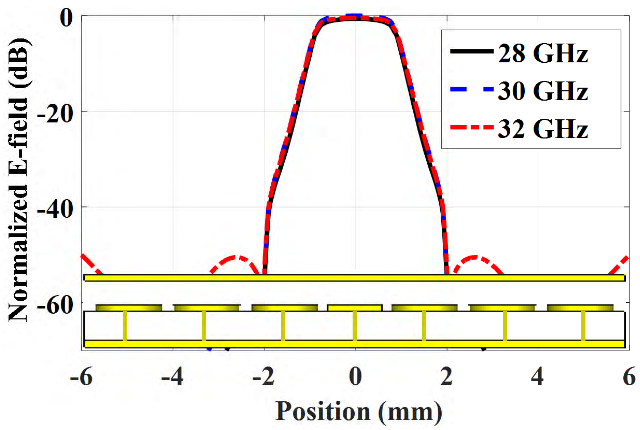

FIGURE 3. Simulated normalized field distribution of the gap waveguide in transverse plane for different frequencies within the operating bandwidth.

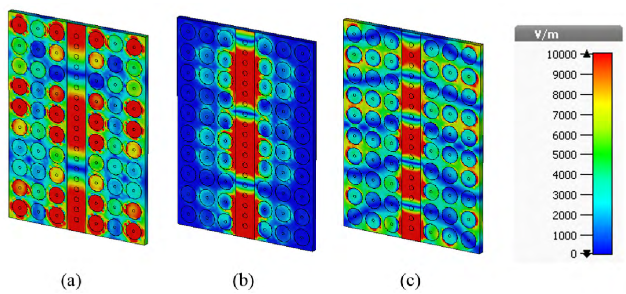

FIGURE 4. The E-field distribution in the PRGW at different frequencies. (a) F = 20 GHz, (b) F = 30 GHz, and (c) F = 40 GHz.

the periodicity of EBG unit cells. This will prevent the signal propagation in the substrate below the microstrip line.

To show the designed cell is able to provide the field confinement above the ridge and suppress any leakage, the field distribution is plotted over the structure which is shown in Figure 3. It is clear that the E-field decays in the order of 60 dB/λ. As a second step of verification, the field distribution is calculated and plotted at different frequency bands in Figure 4. It can be depicted from this figure that the field in confined within the designed band, while the leakage occurs below and above this bandwidth.

B. STRIP LINE MODELING FOR PRGW

Stripline model for the ridge gap wave guide is a useful tool to calculate the characteristic impedance [27]. Assuming an ideal PEC-over-PMC ridge gap waveguide, image theory to

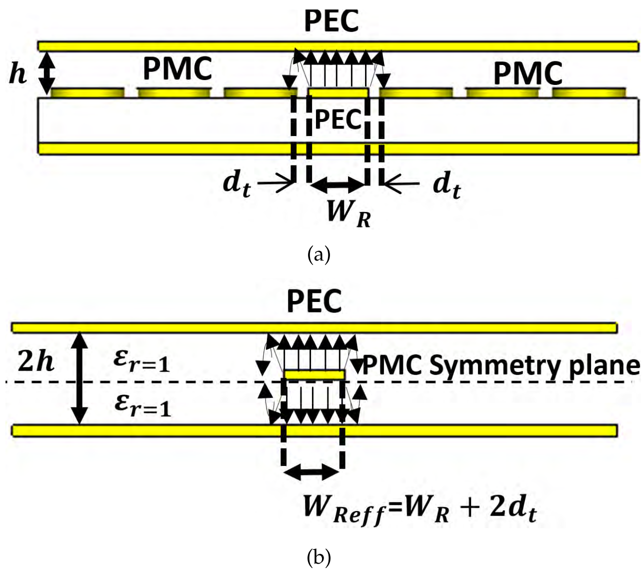

FIGURE 5. Cross-sections of (a) PRGW, and (b) stripline.

the PMC plate can be applied to obtain a stripline model. Figure 5(a) shows the stripline model used for the PRGW. This model considers the RGW as a stripline in a homogeneous medium with dielectric constant ε_r =1 since the EBG mushroom's surface can be modeled as a perfect magnetic conductor as shown in Figure 5(b).

The characteristics impedance Z_o of strip line is given by [30]:

$$Z_o\sqrt{\varepsilon_r} = \begin{cases} 30ln(2\frac{1+\sqrt{k}}{1-\sqrt{k}}), & \text{if } 0 \le k^2 \le 0.5 \\ 30\pi^2(ln(2\frac{1+\sqrt{\sqrt{1-k^2}}}{1-\sqrt{\sqrt{1-k^2}}}))^{-1}, & \text{if } 0.5 \le k^2 \le 1 \end{cases} \tag{1}$$

where, $k = sech(\frac{\pi W_{Reff}}{2\,h})$. In this work, we propose a slight modification that produces a more accurate result for the evaluating the characteristic impedance of the PRGW. Hence, the fringing effect should be considered which makes the effective electrical width of the ridge is wider than its physical width by factor 2 d_t. Therefore, the width of equivalent stripline W_{Reff} is given by:

$$W_{Reff} = W_R + 2d_t \tag{2}$$

Applying the previous equations on different air gap height and minimize the error between the calculated and simulated characteristic impedance for a wide range of ridge width W_R, the incremental factor can be approximately obtained as:

$$d_t = \sum_{i=0}^{3} c_i h^i \tag{3}$$

where, the polynomial coefficients of the previous equation are denoted by c_i (i=0,1,2,3) are equal to 0.02, 0.83, −0.86,

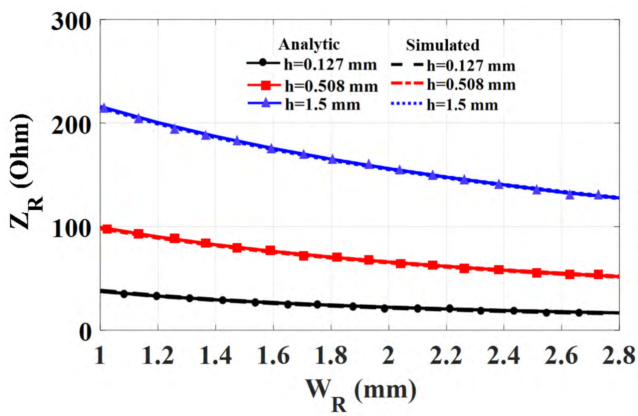

FIGURE 6. The characteristic impedance of PRGW versus the W_R.

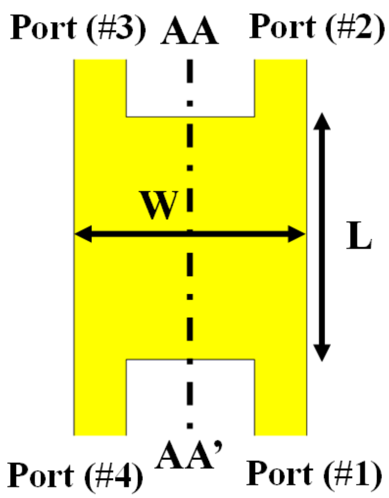

FIGURE 7. Configuration of a four-port rectangle-junction circuit.

and 0.25, respectively. Hence, an accurate value for the characteristic impedance of PRGW Z_R is given by:

$$Z_R = 2Z_o \tag{4}$$

By using the previous equations, the comparison between the calculated Z_R for a PRGW line and the simulated value is shown in Figure 6. The comparison results emphasize on the validity of the strip line model modification proposed in this work. In order to avoid the complexity of the design regarding the arrangement of the mushroom cells around lines, the width of line is chosen to be approximately equal to the EBG unit cell dimension. This way avoids the challenge process to adjust the circuit layout without the need to readjust the mushroom cell's location. Hence, the width of the ridge is selected to be W_R=1.5 mm, where the associated characteristic impedance is Z_R= 79 Ω as the gap height is exactly equal to the selected substrate thickness.

C. PRGW HYBRID COUPLER DESIGN PROCEDURE

Starting with the fact that any arbitrary junction connecting four transmission lines and satisfied certain conditions can work as a directional coupler [31]–[34]. Figure 7 shows a schematic of a four-port rectangular-junction structure with width W and length L. Since this circuit is symmetrical about the plane AA', it can be analyzed through the even/odd mode analysis methodology. Due to the symmetrical and the reciprocal nature of our device, the elements of the scattering matrix of the four port networks, shown in Figure 7, are given as follows [30]:

$$S_{11} = \frac{S_{11}^e + S_{11}^o}{2} \tag{5}$$

$$S_{21} = \frac{S_{21}^e + S_{21}^o}{2} \tag{6}$$

$$S_{31} = \frac{S_{21}^e - S_{21}^o}{2} \tag{7}$$

$$S_{41} = \frac{S_{11}^e - S_{11}^o}{2} \tag{8}$$

where S_{11}^e and S_{11}^o represent the reflection coefficients for the even and odd modes, respectively, while S_{21}^e and S_{21}^o are the transmission coefficients for the even and odd modes, respectively. The circuit can be completely matched under two possibilities. The first one is $S_{11}^e = S_{11}^o = 0$ and the second is $S_{11}^e = -S_{11}^o \neq 0$. Thus, if the field distribution in the connected junction satisfies one of the matching conditions, by optimizing the circuit parameters we can have a directional coupler.

Considering the first condition $S_{11}^e = S_{11}^o = 0$, this leads to having internally matched network at the four ports, where S_{ii}=0, for i=1,2,3 and 4. Moreover, substituting in Equation 8, no coupling occurs between ports 1 and 4, implying that $S_{14} = S_{41} = 0$. Similarly, ports 2 and 3 will be decoupled. This means that the coupler works in the forward coupling mode, which is the objective design in this work.

Considering both the even mode and the odd mode, we have no reflection as $S_{11}^e = S_{11}^o = 0$. As a result the magnitude of the transmission coefficient will be equal to unity $| S_{21}^e |=| S_{21}^o |= 1$, where the circuit is lossless. Hence, in both cases the only difference will be the phase shift, where $S_{21}^e = e^{-j\Phi^e}$ and S_{21}^o= $e^{-j\Phi^o}$,while Φ^e and Φ^o denote the phase difference between port 1 and 2 for the even and odd-mode excitation, respectively. The phase shift can be related to the junction length L with $\Phi^e = \beta^e L$ and $\Phi^o = \beta^o L$, where β^e and β^o represent the propagation constants of the even and odd mode signal. Hence, by using (6) and (8), the scattering parameters of an ideal forward-wave directional coupler are given as follows:

$$S_{21} = \frac{e^{-j\Phi^e} + e^{-j\Phi^o}}{2} \tag{9}$$

$$S_{31} = \frac{e^{-j\Phi^e} - e^{-j\Phi^o}}{2} \tag{10}$$

Thus, the following equation can be derived:

$$S_{21}/S_{31} = -jcot(\frac{\Phi}{2}) \tag{11}$$

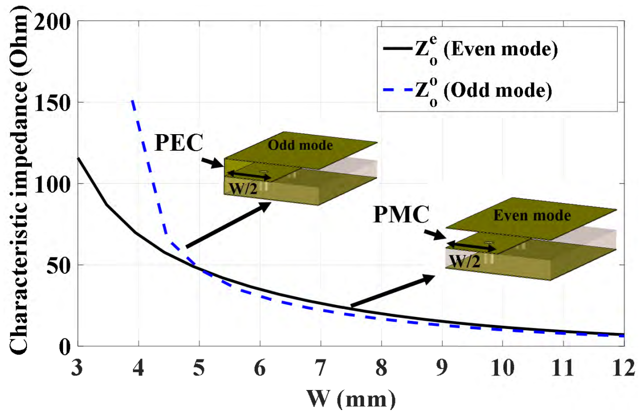

(a)

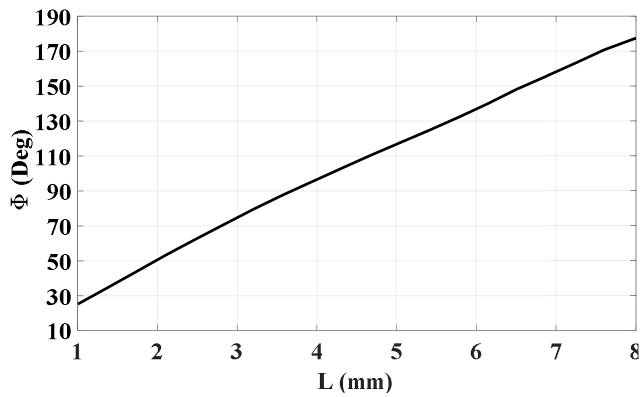

(b)

FIGURE 8. **(a) Characteristics impedances of even and odd modes of a four-port PRGW rectangular-junction. (b) Phase difference in the propagation phase of the even and odd mode.**

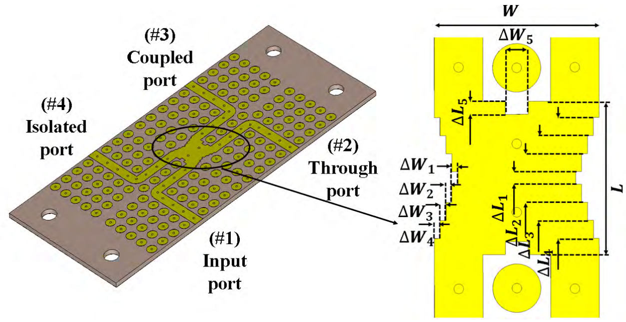

FIGURE 9. **Block diagram of the 3-D geometrical configuration of 3 dB quadrature hybrid coupler (Upper ground is removed for clear illustration).**

TABLE 2. **Final dimensions of the coupling section.**

Dimension		Value in (mm)
Coupling junction length (L)		4.1
Coupling junction width (W)		5
Section1	$\triangle L_1$	0.34
	$\triangle W_1$	0.16
Section2	$\triangle L_2$	1.31
	$\triangle W_2$	0.16
Section3	$\triangle L_3$	2.27
	$\triangle W_3$	0.16
Section4	$\triangle L_4$	3.3
	$\triangle W_4$	0.16
Section5	$\triangle L_5$	0.34
	$\triangle W_5$	0.6

where, $\Phi = (\beta^e - \beta^o)L$. The above equation indicates that the phase difference between the two outputs equals 90°, and the power-split ratio depends on Φ. In addition, the condition for equal power splitting is Φ equal to $\pm 90°$.

Through the even and odd mode analysis, the forward wave coupling condition $S_{11}^e = S_{11}^o = 0$ can be satisfied if $Z_o^e = Z_o^o$,where Z_o^e and Z_o^o are the even and odd mode characteristic impedances for a four-port rectangular-junction structure shown in Figure 7, respectively. The even and odd characteristics impedances for a four-port rectangular-junction integrated in PRGW environment are calculated through applying the magnetic wall (even mode) and electric wall (odd mode) at the plane of symmetry AA'. These impedances are obtained using the CST Microwave Studio simulator for various coupling sections widths W which is plotted in Figure 8(a). It can be noticed that $Z_o^e = Z_o^o$ can be approximately satisfied when $W \geq 5$ mm. From (11), we can notice that the exchange of power between port 2 and 3 of a four port circuit shown in Figure 7 follows up a sinusoidal type profile as a function of coupling section length L. In addition, a 3-dB coupling is realized when Φ equal to $\pm 90°$ and this can be achieved by adjusting the coupling section length L to satisfy that $(\beta^e - \beta^o)L = 90°$. According to the even and odd mode analysis, the phase difference in the propagating phase of the even and odd mode is calculated for the different coupling section length which is plotted in Figure 8(b). The 90° phase difference can be achieved at L= 3.6 mm. Hence, the dimensions obtained through the even and odd mode analysis for the coupling section (W =5 mm and L = 3.6 mm) are considered as initial values for the realization of the proposed coupler. Since $Z_o^e = Z_o^o \neq Z_R$, the coupling section is connected to the PRGW straight lines through matching transformer as shown in Figure 9. Moreover, the coupling section width is designed in the form of multi-steps to add more degrees of freedom that can be used in the fine tuning process. These steps are deployed for mode matching between the quasi TEM mode propagating along the PRGW line and the mode supported by the central section.

D. DESIGN OPTIMIZATION AND RESULTS

The design procedure provided in the previous section is used to obtain the initial dimensions of the coupling section at the design frequency for optimum. The optimization is performed around 10% of the initial dimensions for the design, where the final dimensions are indicated in Table 2. The simulated scattering parameters are shown in Figure 10(a), where the phase difference between the coupled and through port is provided in Figure 10(b). It can be depicted from the simulated results that the realized coupler covers the band from 29 to 31 GHz, which is 6% relative bandwidth at 30 GHz, while the phase imbalance is 85° ±5°. Also, the electric field distribution in Figure 10(c) emphasizes on the performance of the proposed coupler in terms of the isolation.

III. DESIGN OF MICROSTRIP TO PRGW TRANSITION

Transitions between PRGW and microstrip are needed in order to provide the proper excitation. The main objective of the transition is to achieve a sufficient matching level over the operating frequency band of the connected device. The design of microstrip to PRGW transition was well investigated in the literature [26], [28]. These transitions are realized by changing the width of the ridge to match a 50 Ω microstrip line. This technique has fabrication limitations since the via existence at the center of the ridge limits the variation of the ridge width. Hence, another technique is proposed in this work through adding a tapered transition in the microstrip line section to match the ridge gap waveguide impedance as shown in Figure 11 (a) and (b). Hence, the taper transformer should be designed to match the PRGW line impedance Z_R=79 Ω to 50 Ω microstrip line. The tapered transition width is linearly decreased from the 50 Ohm width to a certain width W_t=0.47 mm required to provide the required matching. The length of the transformer L_t is selected to be $\lambda_g/2$ as initial value. Afterwards, an optimization is performed around 5% of the initial dimensions to improve the matching level. The simulated S-parameters of the 90° bend PRGW with the transition is shown in Figure 11 (c). It is clear that the proposed transition achieves a matching level below -15 dB over the frequency band of operation 26-32 GHz, which is sufficient to provide the proper excitation.

IV. EXPERIMENTAL VALIDATION

The fabricated prototype is shown in Figure 12 (a) before performing the assembly to show the details of the three layers forming the proposed coupler. Since connectors and transitions yield more insertion loss, the thru-reflect-line (TRL) calibration is done to de-embed the effects of endlaunch connectors and transitions in measurements. The fabricated microstrip calibration kit is shown in Figure 12 (b) and deployed to perform the calibration of (N52271A) PNA network analyzer. The S-parameters measurement was taken in a sequential way by connecting two ports to the PNA, while the other ports are matched as shown in Figure 12 (c). 3-D printed housing is used to provide a mechanical support and ensure having a robust measurement. This housing is fabricated from a non conducting material that has no effect on the measured results. The measured S-parameters of the proposed coupler are shown in Figure 13(a) demonstrate that the reflection coefficient is below -10 dB from 29 to 31 GHz (6%) with high isolation between ports 1 and 4 at the center operating frequency of 30 GHz. Figure 13(b) shows a 90° phase difference between | S_{21} | and | S_{31} | with a phase imbalance of ±10°. This figure shows a good agreement between simulated and measured results, while the discrepancies between both results may be attributed to the fabrication tolerances and variations in substrate material properties at 30 GHz.

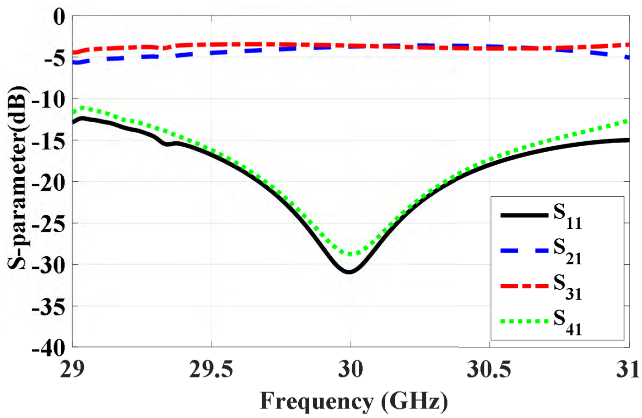

(a)

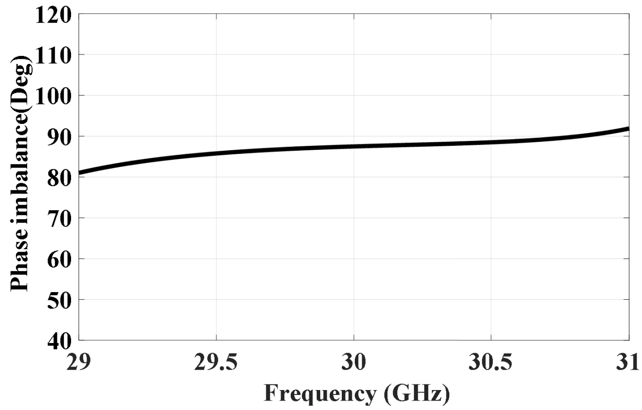

(b)

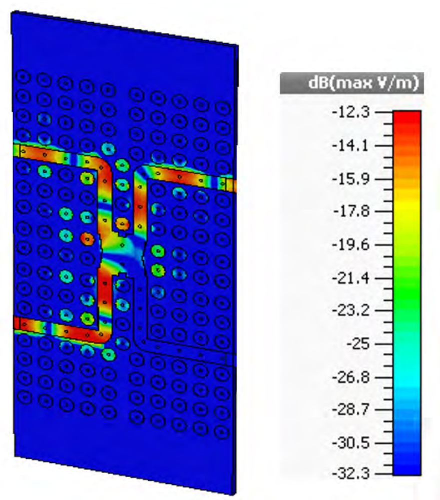

(c)

FIGURE 10. (a) Simulated PRGW hybrid coupler scattering parameters. (b) Phase response of the proposed coupler. (c) The electric field distribution of the proposed coupler.

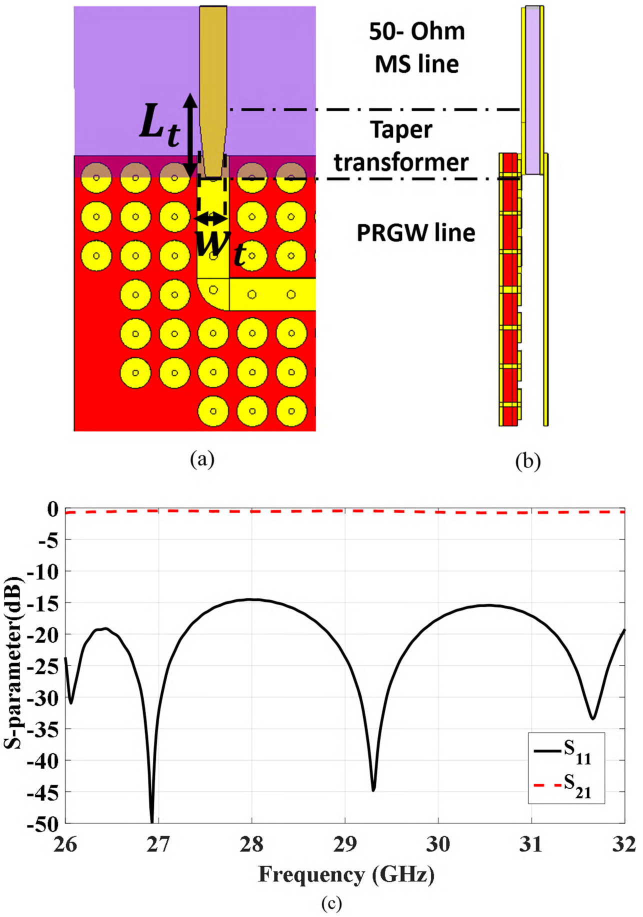

FIGURE 11. Block diagram of 90° bend PRGW with microstrip to PRGW transition. (a) Top view (b) Side view. (c)Simulated S-parameters.

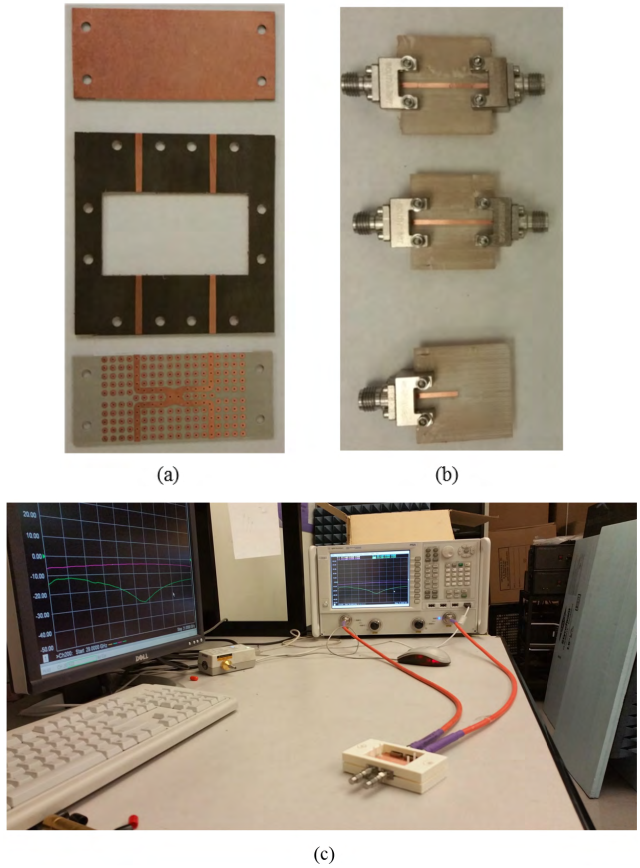

FIGURE 12. (a) Fabrication of the proposed coupler. (b) TRL calibration kits. (c) Measurement setup.

TABLE 3. Comparison between coupler configurations.

	Advantages	Disadvantages
SIW	- Wideband - Better matching - Cheapest fabrication	- High dispersion - Big size - High insertion loss
RGW	- Low dispersion -Low insertion loss - Wideband	- Big size -Expensive fabrication
PRGW	-Low dispersion -Low insertion loss -Small Size	- Narrow band

V. PRGW 3-dB HYBRID COUPLER PERFORMANCE EVALUATION

To evaluate the potential of the proposed structure, the proposed coupler is compared with the other coupling structures implemented with state of art guiding structure technologies such as SIW and RGW. The proposed coupler size is $1.1\lambda_g \times 1.1\ \lambda_g$ at the center frequency. This includes the first two rows of cells around the middle junction. It is implemented based on PRGW technology, which has a superior characteristics at higher frequency bands such as low loss since the waves propagate inside air gap. Moreover, it supports a Q-TEM mode, which results in minimum dispersion supporting wave propagation with minimal distortion. Regarding the electrical specifications, the proposed coupler has a 6% relative bandwidth at 30 GHz. Moreover, it has a quadrature phase shift between the output ports with ± 10 ° over the entire frequency band of 29 to 31 GHz.

Several hybrid coupler configurations were presented in the literature based on SIW technology. The traditional short-slot SIW hybrid coupler has been proposed in many articles before [14], [15]. They have an average size of of $2.5\lambda_g \times 1.3\ \lambda_g$ with relative bandwidth between 3-13 % percentage bandwidth. In addition, the dominant mode is a TE mode, which has more dispersion. Furthermore, SIW has a large insertion loss which exceeds 1 dB due to dielectric losses [14]. Other coupler designs were introduced based on air filled SIW (AFSIW) technology [17]. In this case, the losses decreased closer to the PRGW. The bandwidth is relatively wide which is exceeding 10 % at the expense of the complex fabrication process.

Some other designs using RGW technology have been proposed to decrease the overall loss and support signal transmission with minimal dispersion [24]. The size of this coupler is $1.6\lambda_g \times 1.6\ \lambda_g$ with a percentage bandwidth of 14%. Although this coupler achieves low loss and high power

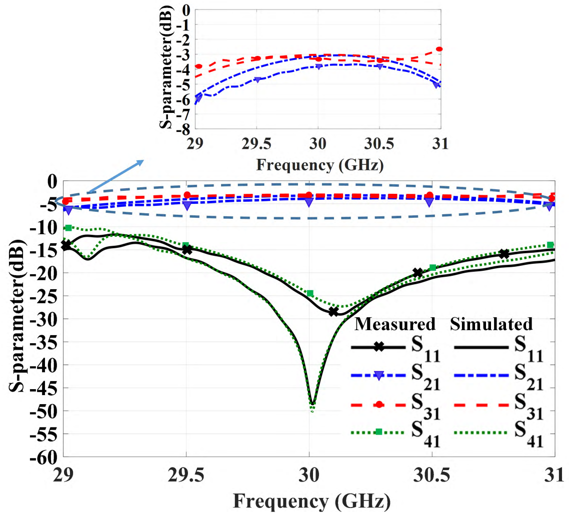

(a)

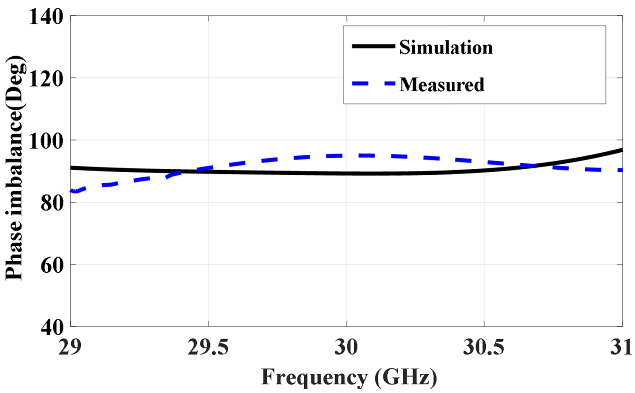

(b)

FIGURE 13. (a) Simulated and measured S-parameters of 3dB quadrature hybrid coupler. (b) Phase response of the proposed coupler.

handling, but it has a big size and utilized an expensive fabrication process. Hence, it is difficult to integrate with monolithic microwave integrated circuit. On the other hand, the proposed coupler is printed on a substrate which can be integrated with other planner circuit. This comparison is summarized in Table 3 to state the characteristics of various configurations and highlights both the advantages and the disadvantages.

VI. Conclusion

Printed ridge gap waveguide forward coupler has been proposed. A systematic design approach of the coupler has been presented and illustrated. The transition from the microstrip line to PRGW is designed based on tapered microstrip line matching section. The prototype of the proposed coupler has been validated the operation in the objective frequency band 29-31 GHz. The measured results show a good agreement with the simulated results. The proposed coupler has promising electrical characteristics that meet the future 5G required specifications.

REFERENCES

[1] Y. Wang, J. Li, L. Huang, Y. Jing, A. Georgakopoulos, and P. Demestichas, "5G mobile: Spectrum broadening to higher-frequency bands to support high data rates," *IEEE Veh. Technol. Mag.*, vol. 9, no. 3, pp. 39–46, Sep. 2014.

[2] *IMT Vision—Framework and Overall Objectives of the Future Development of IMT for 2020 and Beyond*, document Rec. ITU-R M.2083-0, Jul. 2015.

[3] Federal Communications Commission, "FCC takes steps to facilitate next generation wireless technologies in spectrum above 24 GHz," Wireless Telecommun., Int., Eng. Technol., Washington, DC, USA, Tech. Rep. 20554, Jul. 2016.

[4] T. S. Rappaport, J. N. Murdock, and F. Gutierrez, Jr., "State of the art in 60-GHz integrated circuits and systems for wireless communications," *Proc. IEEE*, vol. 99, no. 8, pp. 1390–1436, Aug. 2011.

[5] S. I. Shams, M. Elsaadany, G. Saad, and A. A. Kishk, "Compact wideband dual loop coupler with high power handling capability for radar applications," *IEEE Microw. Compon. Lett.*, vol. 27, no. 10, pp. 900–902, Oct. 2017.

[6] H.-L. Ting, S.-K. Hsu, and T.-L. Wu, "A novel and compact eight-port forward-wave directional coupler with arbitrary coupling level design using four-mode control technology," *IEEE Trans. Microw. Theory Techn.*, vol. 65, no. 2, pp. 467–475, Feb. 2017.

[7] X. Shen, Y. Liu, S. Zhou, and Y. Wu, "Coupled-line directional coupler with tunable power division ratio and operating frequency," *IET Microw., Antennas Propag.*, vol. 11, no. 1, pp. 59–68, Jan. 2017.

[8] W. M. Fathelbab, "The synthesis of a class of branch-line directional couplers," *IEEE Trans. Microw. Theory Techn.*, vol. 56, no. 8, pp. 1985–1994, Aug. 2008.

[9] R. Gomez-Garcia, J. I. Alonso, and D. Amor-Martin, "Using the branch-line directional coupler in the design of microwave bandpass filters," *IEEE Trans. Microw. Theory Techn.*, vol. 53, no. 10, pp. 3221–3229, Oct. 2005.

[10] A. Doghri, T. Djerafi, A. Ghiotto, and K. Wu, "Substrate integrated waveguide directional couplers for compact three-dimensional integrated circuits," *IEEE Trans. Microw. Theory Techn.*, vol. 63, no. 1, pp. 209–221, Jan. 2015.

[11] T. Djerafi and K. Wu, "Super-compact substrate integrated waveguide cruciform directional coupler," *IEEE Microw. Wireless Compon. Lett.*, vol. 17, no. 11, pp. 757–759, Nov. 2007.

[12] Z. Liu and G. Xiao, "Local design of SIW-based multi-aperture couplers using ray tracing method," *IEEE Trans. Compon., Packag., Manuf. Technol.*, vol. 7, no. 1, pp. 106–113, Jan. 2017.

[13] B. Liu, W. Hong, Z. C. Hao, and K. Wu, "Substrate integrated waveguide 180-degree narrow-wall directional coupler," in *Proc. Asia–Pacific Microw. Conf.*, Dec. 2005, pp. 1–3.

[14] L. Han, K. Wu, X.-P. Chen, and F. He, "Accurate and efficient design technique for wideband substrate integrated waveguide directional couplers," *Int. J. RF Microw. Comput.-Aided Eng.*, vol. 22, no. 2, pp. 248–259, Mar. 2012.

[15] W. M. Abdel-Wahab and S. Safavi-Naeini, "Low loss H-shape SIW hybrid coupler for millimeter-wave phased arrays antenna systems," in *Proc. IEEE Antennas Propag. Soc. Int. Symp. (APS/URSI)*, Jul. 2012, pp. 1–2.

[16] B. Liu, W. Hong, Y. Zhang, H. J. Tang, X. Yin, and K. Wu, "Half mode substrate integrated waveguide 180° 3-dB directional couplers," *IEEE Trans. Microw. Theory Techn.*, vol. 55, no. 12, pp. 2586–2592, Dec. 2007.

[17] F. Parment, A. Ghiotto, T. P. Vuong, J. M. Duchamp, and K. Wu, "Air-filled substrate integrated waveguide for low-loss and high power-handling millimeter-wave substrate integrated circuits," *IEEE Trans. Microw. Theory Techn.*, vol. 63, no. 4, pp. 1228–1238, Apr. 2015.

[18] T. R. Jones and M. Daneshmand, "The characterization of a ridged half-mode substrate-integrated waveguide and its application in coupler design," *IEEE Trans. Microw. Theory Techn.*, vol. 64, no. 11, pp. 3580–3591, Nov. 2016.

[19] P.-S. Kildal, E. Alfonso, A. Valero-Nogueira, and E. Rajo-Iglesias, "Local metamaterial-based waveguides in gaps between parallel metal plates," *IEEE Antennas Wireless Propag. Lett.*, vol. 8, no. 4, pp. 84–87, Apr. 2009.

[20] H. Raza, J. Yang, P.-S. Kildal, and E. A. Alós, "Microstrip-ridge gap waveguide-study of losses, bends, and transition to WR-15," *IEEE Trans. Microw. Theory Techn.*, vol. 62, no. 9, pp. 1943–1952, Sep. 2014.

[21] E. Alfonso, M. Baquero, P.-S. Kildal, A. Valero-Nogueira, E. Rajo-Iglesias, and J. I. Herranz, "Design of microwave circuits in ridge-gap waveguide technology," in *IEEE MTT-S Int. Microw. Symp. Dig.*, Anaheim, CA, USA, May 2010, pp. 1544–1547.

[22] S. I. Shams, M. M. Tahseen, and A. A. Kishk, ''Wideband relative permittivity characterization of thin low permittivity textile materials based on ridge gap waveguides,'' *IEEE Trans. Microw. Theory Techn.*, vol. 64, no. 11, pp. 3839–3850, Nov. 2016.
[23] S. I. Shams, M. A. Abdelaal, and A. A. Kishk, ''Broadside uniform leaky-wave slot array fed by ridge gap splitted line,'' in *Proc. IEEE Antennas Propag. Soc. Int. Symp. (APS/URSI)*, Vancouver, BC, Canada, Jul. 2015, pp. 2467–2468.
[24] S. I. Shams and A. A. Kishk, ''Design of 3-dB hybrid coupler based on RGW technology,'' *IEEE Trans. Microw. Theory Techn.*, vol. 65, no. 10, pp. 3849–3855, Oct. 2017.
[25] S. A. Razavi, P. S. Kildal, L. Xiang, E. Alfonso Alos, and H. Chen, ''2×2-slot element for 60-GHz planar array antenna realized on two doubled-sided PCBs using SIW cavity and EBG-type soft surface fed by microstrip-ridge gap waveguide,'' *IEEE Trans. Antennas Propag.*, vol. 62, no. 9, pp. 4564–4573, Sep. 2014.
[26] M. Sharifi Sorkherizi and A. A. Kishk, ''Transition from microstrip to printed ridge gap waveguide for millimeter-wave application,'' in *Proc. IEEE Antennas Propag. Soc. Int. Symp. (APS/URSI)*, Vancouver, BC, Canada, Jul. 2015, pp. 1588–1589.
[27] A. Polemi and S. Maci, ''Closed form expressions for the modal dispersion equations and for the characteristic impedance of a metamaterial-based gap waveguide,'' *IET Microw., Antennas Propag.*, vol. 4, no. 8, pp. 1073–1080, Aug. 2010.
[28] A. U. Zaman, T. Vukusic, M. Alexanderson, and P.-S. Kildal, ''Design of a simple transition from microstrip to ridge gap waveguide suited for MMIC and antenna integration,'' *IEEE Antennas Wireless Propag. Lett.*, vol. 12, pp. 1558–1561, 2013.
[29] S. I. Shams and A. A. Kishk, ''Printed texture with triangle flat pins for bandwidth enhancement of the ridge gap waveguide,'' *IEEE Trans. Microw. Theory Techn.*, vol. 65, no. 6, pp. 2093–2100, Jun. 2017.
[30] R. Mongia, I. J. Bahl, P. Bhartia, and S. J. Hong, *RF and Microwave Coupled-line Circuits*. Norwood, MA, USA: Artech House, 2007.
[31] C. G. Montgomery, and H. Robert, M. Edward, ''Principles of microwave circuits,'' in *Peter Peregrinus on Behalf of the Institution of Electrical Engineers*. London, U.K.: IET, 1987.
[32] S. Y. Zheng, J. H. Deng, Y. M. Pan, and W. S. Chan, ''Circular sector patch hybrid coupler with an arbitrary coupling coefficient and phase difference,'' *IEEE Trans. Microw. Theory Techn.*, vol. 61, no. 5, pp. 1781–1792, May 2013.
[33] K.-L. Chan, F. A. Alhargan, and S. R. Judah, ''A quadrature-hybrid design using a four-port elliptic patch,'' *IEEE Trans. Microw. Theory Techn.*, vol. 45, no. 2, pp. 307–310, Feb. 1997.
[34] T. Kawai and I. Ohta, ''Planar-circuit-type 3-dB quadrature hybrids,'' *IEEE Trans. Microw. Theory Techn.*, vol. 42, no. 12, pp. 2462–2467, Dec. 1994.

MOHAMED MAMDOUH M. ALI (S'15) received the B.Sc. (Hons.) and M.Sc. degrees in electronics and communications engineering from Assiut University, Egypt, in 2010 and 2013, respectively. He is currently pursuing the Ph.D. degree in electrical and computer engineering from Concordia University, Montréal, Québec, Canada, in 2016. From 2010 to 2015, he was a Teaching and Research Assistant with the Department of Electronics and Communications Engineering, Assiut University. He was a Teaching and Research Assistant with Concordia University. His current research interests include microwave reciprocal/nonreciprocal design and analysis and antenna design.

SHOUKRY I. SHAMS (M'04) received the B.Sc. (Hons.) and M.Sc. degrees in electronics and communications engineering from Cairo University, Egypt, in 2004 and 2009, respectively, the Ph.D. degree in electrical and computer engineering from Concordia University, Montréal, Québec, Canada, in 2016.

From 2005 to 2006, he served as a Teaching and Research Assistant with the Department of Electronics and Communications Engineering, Cairo University. From 2006 to 2012, he served as a Teaching and Research Assistant with the IET Department, German University in Cairo. From 2012 to 2016, he was a Teaching and Research Assistant with Concordia University. His research interests include microwave reciprocal/nonreciprocal design and analysis, high power microwave subsystems, antenna design, and material measurement.

Dr. Shams received the Faculty Certificate of Honor in 1999, The Distinction with Honor in 2004 from Cairo University. He was a recipient of the Concordia University Recruitment Award in 2012 and Concordia University Accelerator Award in 2016. He was the GUC-IEEE Student Branch Chair from 2010 to 2012.

ABDEL-RAZIK SEBAK (F'10) received the B.Sc. degree (Hons.) in electrical engineering from Cairo University, Cairo, Egypt, in 1976, the B.Sc. degree in applied mathematics from Ain Shams University, Cairo, in 1978, and the M.Eng. and Ph.D. degrees in electrical engineering from the University of Manitoba, Winnipeg, MB, Canada, in 1982 and 1984, respectively. From 1984 to 1986, he was with Canadian Marconi Company, involved in the design of microstrip phased array antennas. From 1987 to 2002, he was a Professor with the Department of Electronics and Communication Engineering, University of Manitoba. He is currently a Professor with the Department of Electrical and Computer Engineering, Concordia University, Montréal, Québec, Canada. His research interests include phased array antennas, millimeter-wave antennas and imaging, computational electromagnetics, and interaction of EM waves with engineered materials and bio electromagnetics. He is a member of the Canadian National Committee of International Union of Radio Science Commission B. He was a recipient of the 2000 and 1992 University of Manitoba Merit Award for outstanding Teaching and Research, the 1994 Rh Award for Outstanding Contributions to Scholarship and Research, and the 1996 Faculty of Engineering Superior. He has served as the Chair of the IEEE Canada Awards and Recognition Committee from 2002 to 2004, and as the Technical Program Chair of the 2002 IEEE CCECE Conference and the 2006 URSIANTEM Symposium. He is the Technical Program Co-Chair for the 2015 IEEE ICUWB Conference.